Structures of protective antibodies reveal sites of vulnerability on Ebola virus

Charles D. Murin[a,b], Marnie L. Fusco[b], Zachary A. Bornholdt[b], Xiangguo Qiu[c], Gene G. Olinger[d], Larry Zeitlin[e], Gary P. Kobinger[c,f,g], Andrew B. Ward[a,1], and Erica Ollmann Saphire[b,h,1]

[a]Department of Integrative Structural and Computational Biology, [b]Department of Immunology and Microbial Science, and [h]The Skaggs Institute for Chemical Biology, The Scripps Research Institute, La Jolla, CA 92037; [c]National Microbiology Laboratory, Public Health Agency of Canada, Winnipeg, MB, Canada R3E 3R2; [d]National Institute of Allergy and Infectious Diseases/Integrated Research Facility, National Institutes of Health, Frederick, MD 21702; [e]Mapp Biopharmaceutical, San Diego, CA 92121; [f]Department of Medical Microbiology, University of Manitoba, Winnipeg, MB, Canada R3E 0J9; and [g]Department of Immunology, University of Manitoba, Winnipeg, MB, Canada R3E 0T5

Edited by Peter Palese, Icahn School of Medicine at Mount Sinai, New York, NY, and approved October 22, 2014 (received for review July 31, 2014)

Ebola virus (EBOV) and related filoviruses cause severe hemorrhagic fever, with up to 90% lethality, and no treatments are approved for human use. Multiple recent outbreaks of EBOV and the likelihood of future human exposure highlight the need for pre- and postexposure treatments. Monoclonal antibody (mAb) cocktails are particularly attractive candidates due to their proven postexposure efficacy in nonhuman primate models of EBOV infection. Two candidate cocktails, MB-003 and ZMAb, have been extensively evaluated in both in vitro and in vivo studies. Recently, these two therapeutics have been combined into a new cocktail named ZMapp, which showed increased efficacy and has been given compassionately to some human patients. Epitope information and mechanism of action are currently unknown for most of the component mAbs. Here we provide single-particle EM reconstructions of every mAb in the ZMapp cocktail, as well as additional antibodies from MB-003 and ZMAb. Our results illuminate key and recurring sites of vulnerability on the EBOV glycoprotein and provide a structural rationale for the efficacy of ZMapp. Interestingly, two of its components recognize overlapping epitopes and compete with each other for binding. Going forward, this work now provides a basis for strategic selection of next-generation antibody cocktails against Ebola and related viruses and a model for predicting the impact of ZMapp on potential escape mutations in ongoing or future Ebola outbreaks.

Ebola | ZMapp | EM | antibodies

Ebolaviruses cause extremely lethal hemorrhagic fever. Since first identified in 1976 (1), there have been at least 20 major human outbreaks in Africa, the most recent of which has caused more than 8,000 cases and more than 4,000 deaths (as of October 10, 2014, World Health Organization). Further, the Reston species of ebolavirus, lethal to nonhuman primates (NHPs) (2) and other animals, is prevalent in Asia and has resulted in large-scale culling of swine farms (3, 4).

Several candidate therapeutics against Ebola virus (EBOV) are currently being evaluated, including postexposure vaccines (5–10), small molecule inhibitors (11–13), siRNA-based therapeutics (14, 15), and mAbs (16–18). Passive administration of mAbs offers an extended treatment window and has proven highly efficacious in NHPs (19–24). Such mAbs could serve as a therapeutic for occupational or natural infection, either prophylactically or after exposure or infection. Initial studies of protective mAbs in rodent models showed that there was a synergistic effect when antibodies are combined, increasing the potency of protection. There were no major differences in protection whether three or five antibodies are combined (25, 26), and antibody cocktails have since generally consisted of no more than three antibodies. Key components of two of the most efficacious mAbs cocktails, titled MB-003 (MappBio) including antibodies c13C6, h13F6, and c6D8 (27) and ZMAb (Defyrus) including antibodies c1H3, c2G4, and c4G7 (22), have been recently combined and are being developed for human use as a cocktail named ZMapp (24). The mAb components of ZMapp include c13C6, c2G4, and c4G7. Each of these antibodies was raised in vaccinated mice (28, 29), chimerized into human IgG1 scaffolds (21, 27, 30, 31), and are currently being mass produced in tobacco plants (31).

A major knowledge gap is the current lack of information regarding the epitopes of these and other mAbs and their mechanism of action. In 1999, a neutralizing mAb KZ52 was isolated from a human survivor (32). KZ52 protected mice and guinea pigs from lethal infection (33), but failed to protect NHPs when delivered as a single mAb, in two dosages at 1 day before and 4 days after infection (34). The failure of this single mAb delivered alone made it unclear, at the time, if neutralizing antibodies could confer protection against EBOV infection. Results have since shown that the presence of antibody does correlate with protection (35) and that several combinations of different mAbs do confer postexposure protection of NHPs (19–24). Therefore, it remains an open question if the failure of KZ52 was because of some inadequacy of its epitope or function or because it was delivered as a single mAb.

A combination of two or more antibodies may confer protection via complementary mechanisms, involving neutralization and neutralization-independent mechanisms and may reduce the

Significance

Ebola virus causes lethal hemorrhagic fever, and the current 2014 outbreak in western Africa is the largest on record to date. No vaccines or therapeutics are yet approved for human use. Therapeutic antibody cocktails, however, have shown efficacy against otherwise lethal Ebola virus infection and show significant promise for eventual human use. Here we provide structures of every mAb in the ZMapp cocktail, as well as additional antibodies from the MB-003 and ZMAb cocktails from which ZMapp was derived, each in complex with the Ebola glycoprotein. The set of structures illustrates sites of vulnerability of Ebola virus, and importantly, provides a roadmap to determine their mechanism of protection and for ongoing selection and improvement of immunotherapeutic cocktails against the filoviruses.

Author contributions: C.D.M., M.L.F., Z.A.B., A.B.W., and E.O.S. designed research; C.D.M. and M.L.F. performed research; X.Q., G.G.O., L.Z., and G.P.K. contributed new reagents/analytic tools; C.D.M., M.L.F., Z.A.B., X.Q., G.G.O., L.Z., G.P.K., A.B.W., and E.O.S. analyzed data; and C.D.M., A.B.W., and E.O.S. wrote the paper.

The authors declare no conflict of interest.

This article is a PNAS Direct Submission.

Data deposition: EM reconstructions have been deposited in the Electron Microscopy Data Bank, www.emdatabank.org (accession nos. EMDB 6150–6153).

[1]To whom correspondence may be addressed. Email: abward@scripps.edu or erica@scripps.edu.

This article contains supporting information online at www.pnas.org/lookup/suppl/doi:10.1073/pnas.1414164111/-/DCSupplemental.

opportunity for selection of escape mutants. Two of the antibodies in the ZMAb cocktail (c4G7 and c2G4) are neutralizing, whereas the third (c1H3) is nonneutralizing (22, 26, 36). None of the MB-003 mAbs are neutralizing in the absence of complement (29), but both ZMAb and MB-003 mixtures are protective (22, 27). Nonneutralizing antibodies could confer in vivo protection by preventing budding of nascent virions, as has been proposed for Marburg virus (37), or by conferring antibody-dependent cellular cytotoxicity or another immune mechanism. For EBOV, antibodies against the mucin-like domains of the glycoprotein (GP) are generally nonneutralizing because these domains, as well as any antibodies bound to them, are stripped from the viral surface by host cathepsins in the endosome, leaving behind an antibody-free, functional receptor-binding core of GP (16, 38).

By contrast, the epitopes of antibodies against the base of GP, including KZ52 (39) and the anti-Sudan virus (SUDV) antibody 16F6 (38), do neutralize infection in vitro, because they are unaffected by cathepsin cleavage or the low pH of the endosome. KZ52 and 16F6 simultaneously bind both the GP1 and GP2 subunits of GP in their prefusion complex and may neutralize Ebola virus by preventing the conformational rearrangements of GP that drive membrane fusion (38, 39).

We sought to identify the binding sites of each conformational antibody contained in the highly efficacious MB-003 and ZMAb cocktails and subsequently a structure of the reformulated ZMapp cocktail as well. MB-003 contains antibodies c13C6, which binds the GP core, as well as c13F6 and c6D8, which both bind to previously characterized linear epitopes in the mucin-like domain (29, 40). ZMAb contains antibodies c1H3, c2G4, and c4G7, all of which bind the GP core. ZMapp contains c13C6, c2G4, and c4G7 (24). Here, we present single-particle EM reconstructions of recombinantly expressed, soluble, and fully glycosylated Ebola GP ectodomain (GPΔTM) in complex with the fragment antigen binding (Fabs) of the four antibodies that bind to regions outside the mucin-like domain: c13C6 from MB-003 and c1H3, c2G4, and c4G7 from ZMAb/ZMapp. These structures and additional competition data indicate that c13C6 and c1H3 bind overlapping epitopes in the glycan cap and compete and that c2G4 and c4G7 bind overlapping epitopes in the base and also compete. The c2G4/c4G7 site further overlaps with that of human KZ52 and murine 16F6. The resulting body of data demonstrates that neutralizing antibodies (38) and nonneutralizing but protective antibodies collectively target particular regions on GP, irrespective of their source or method of elicitation. These data suggest the mechanisms of protection imparted by these mAbs and provide a roadmap for functional analysis. Further, our work builds a framework by which other protective mAbs can be mapped, and offers direction for development of a next-generation monoclonal antibody therapy against Ebola and similar viruses.

Results

Binding Competition Analysis by Biolayer Interferometry. The GP1 or GP2 subunit bound by each antibody of the MB-003 and ZMAb cocktails has previously been reported: (*i*) h13F6 and c6D8 both bind linear epitopes within the GP1 mucin-like domains (29), (*ii*) c1H3 and c13C6 bind to quaternary epitopes within a region in GP1 that is shared between GP and sGP (28, 29), and (*iii*) c2G4 and c4G7 bind quaternary epitopes on the GP trimer, with c2G4 mostly recognizing GP2 and c4G7 recognizing a portion of GP1 (28). Further, point mutants that lead to escape from c1H3 lie at the top of GP1 in the vicinity of the glycan cap, whereas those for c2G4 and c4G7 lie near the GP1–GP2 interface (22). Here we used biolayer interferometry (BLI) to compare the binding of each of these antibodies side-by-side in a single assay (Fig. 1). A GP ectodomain, which is fully glycosylated and contains the mucin-like domains, but lacks the transmembrane (TM) region (GPΔTM), was engineered with a double strep-tag at the C terminus, near the site of the entry into the viral membrane. The position of this tag likely mimics the orientation of GP on the viral surface to allow proper exposure of relevant epitopes while bound to the sensor. Biosensors coated with GPΔTM were first saturated with 1 μM of antibody 1 before saturation with the same concentration of antibody 2. mAbs were considered to be competing for the same site if maximum binding of antibody 2 was reduced to <10% of its noncompeted binding (black boxes with white numbers). mAbs were considered noncompetitive if maximum binding of antibody 2 was >30% of its binding to GP alone (white boxes with red numbers). Gray boxes with black numbers indicate an intermediate phenotype (between 10% and 30% of uncompeted binding) (Fig. 1).

Analysis of the competition data revealed that the antibodies bind to three general areas on GP, which we divide into three groups (Fig. 1 and Fig. S1). Group 1 contains c4G7 and c2G4, which strongly compete, suggesting that these two antibodies' epitopes significantly overlap. Group 2 contains c13C6 and c1H3. Binding of c13C6 strongly blocks binding of c1H3, suggesting that these antibodies' epitopes overlap as well. Binding of c1H3 diminishes but does not completely block binding of c13C6. Retention of some c13C6 binding even after binding of c1H3 is likely due to incomplete saturation of GP by c1H3. Group 3, containing h13F6 and c6D8, corresponds to the mucin-like domain. Both antibodies bind this domain, but the two antibodies do not compete with each other. The linear epitopes of these antibodies have previously been determined (residues 405–413 for 13F6 and residues 389–405 for 6D8) (29), and a crystal structure of 13F6 in complex with its peptide epitope exists (40). These linear epitopes are either

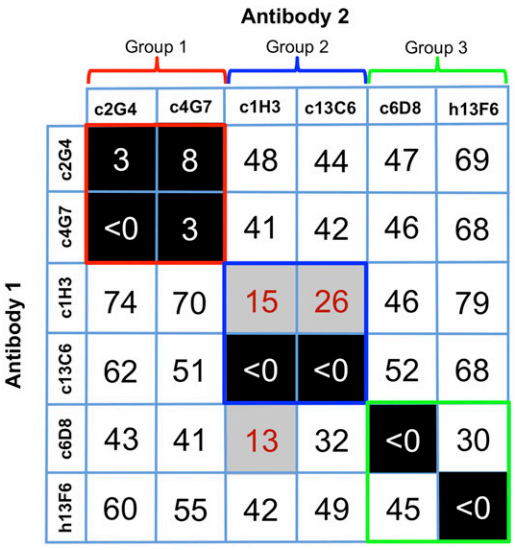

Fig. 1. Competition binding assays. Antibodies from the anti-Ebola cocktails MB-003 and ZMAb were compared for their binding to Ebola GPΔTM to determine if there were any overlapping binding sites within or between mAb cocktails. The percent binding of the competing mAb in the presence of the first mAb was determined by comparing the maximal signal of competing mAb applied after the first mAb complex to the maximal signal of competing mAb alone. MAbs were considered competing for the same site if maximum binding of antibody 2 was reduced to <10% of its binding to GP alone (black boxes with white numbers). mAbs were considered noncompetitive if maximum binding of antibody 2 was >30% of its binding to GP alone (white boxes with black numbers). Gray boxes with red numbers indicate an intermediate phenotype (between 10% and 30% of its binding to GP alone).

physically separate in 3D space, or the mucin domain is flexible enough to prevent significant overlap in the context of the tertiary complex. These data also support the current model of the mucin-like domain as a physically separate portion of GP1, likely extending outward from the top of GP (39, 41), because no mucin-like domain antibody in this study inhibits binding of any antibody against the remaining core of GP.

Single-Particle EM Structures of c13C6, c2G4, c4G7, and c1H3 Fabs Bound to Mucin-Containing Ebola GP. To determine the epitopes and locate each competition group in the context of GP, single-particle EM was used to generate reconstructions of the conformational antibody Fabs in the MB-003 and ZMAb cocktails in complex with GPΔTM, (Fig. 2 *A*–*D*, Figs. S2 and S3 *A* and *B*, and Table S1). Fabs were added in 10-molar excess to GP and purified by size-exclusion chromatography (SEC) before subsequent staining and reconstruction by single-particle EM. These structures allowed us to make a hybrid map of the ZMapp cocktail (24), which is composed of c13C6 from MB-003 and c2G4 and c4G7 from ZMAb (Fig. 2*E* and Fig. S3*C*).

The structure of the c13C6-GP complex shows that the antibody binds perpendicularly to the expected plane of the membrane, straight down onto the surface of the GP, in the region of the glycan cap (Fig. 2*A* and Fig. S2*A*). To verify the binding site of c13C6 relative to the GP, we also added antibody KZ52, for which the crystal structure bound to mucin-deleted GP has already been determined (39). KZ52 binds the base of GP, not the glycan cap, and serves as an internal validation in our structure for the binding site of c13C6 (Fig. S2*A*).

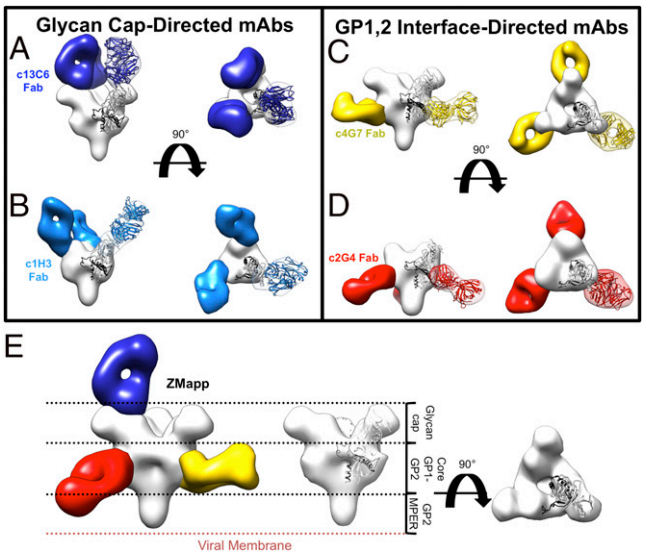

Fig. 2. Single-particle negative-stain EM reconstructions of MB-003 and ZMAb antibodies bound to EBOV GPΔTM. Hybrid models of negative-stain EM reconstructions fit with the EBOV GPΔmuc crystal structure (PDB ID code 3CSY) (39) with GP1 in white and GP2 in black. Core GPs and Fabs are rendered as surfaces with GPs in white and Fabs in various colors. Fab densities are fit with a model Fab structure for reference. (*A*) Fab c13C6 (in dark blue) and KZ52 (removed) in complex with EBOV GPΔTM showing side (*Left*) and top (*Right*) views of the reconstruction. (*B*) Fab c1H3 (in light blue) and KZ52 (removed) in complex with EBOV GPΔTM showing side (*Left*) and top (*Right*) views of the reconstruction. (*C*) Fab c4G7 (in yellow) and c13C6 (removed) in complex with EBOV GPΔTM showing side (*Left*) and top (*Right*) views of the reconstruction. (*D*) Fab c2G4 (red) in complex with EBOV GPΔTM showing side (*Left*) and top (*Right*) views of the reconstruction. (*E*) Side view comparisons of liganded EBOV GPΔTM (*Left*, hybrid reconstruction of GPΔTM in complex with c4G7 in yellow, c13C6 in blue, c2G4 in red, and GP in white) and unliganded GPΔTM (*Center* and *Right*, Fabs removed). Relative positions of domains on GP are indicated.

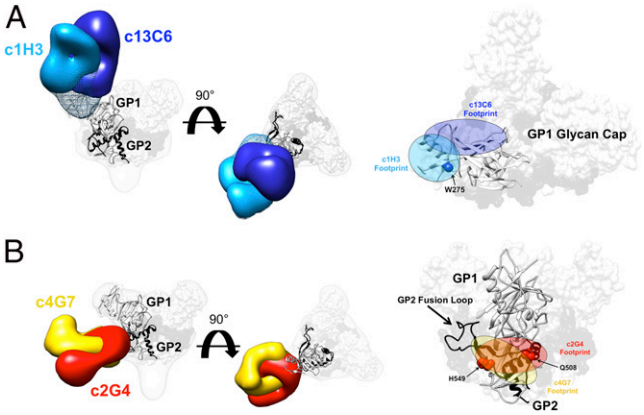

Fig. 3. Details of the glycan cap and GP1-GP2 interface epitopes. (*A*) Competition analysis indicated that antibodies c13C6 and c1H3 have overlapping epitopes. Here, structures of c13C6 (dark blue) and c1H3 (light blue) bound to GPΔTM are illustrated, with the GPΔmuc crystal structure (PDB ID code 3CSY) fit into the GP EM density. GP1 is white and GP2 is black. Superimposition of the structures illustrates that the antibodies have overlapping epitopes within the glycan cap on GP1 (side view on the far left, top view in the center and far right). The footprints of these antibodies are highlighted on the far right. The mesh portion of the reconstruction is the part of the GP glycan cap that is resolved in the c1H3:GPΔTM structure. (*B*) As in *A* but c4G7 is in yellow and c2G4 is in red (side view on the far left and right, top view in the center).

The mucin-like domains comprise nearly half the mass of GP and are thought to be heavily glycosylated and disordered (39, 41–44). Notably, these domains are not visible in our class averages (Fig. S2), due to their flexibility and poor negative-stain compatibility. Further, the anti-mucin mAbs h13F6 and c6D8 were not resolved in complex with GP, also likely due to this flexibility. In an effort to reduce flexibility, complexes of h13F6 and c6D8 Fabs with GPΔTM were lightly fixed with 0.125% glutaraldehyde before imaging. In the class averages of the fixed particles, the Fabs were poorly resolved (Fig. S4), but are weakly visible near the top of GP. The structure of another mucin-like domain antibody, 14G7 (44), bound to viral particles has previously been attempted by cryo-tomography. Similarly, the Fab density was unable to be resolved due to significant flexibility, although at least a portion of the mucin-like domain was visualized extending away from the glycan cap on GP (41).

All three mAbs from the ZMAb mixture are against the GP core, outside the mucin-like domain, and could be structurally characterized by negative-stain EM. We added the noncompeting Fabs KZ52 and c13C6 to the c1H3 and c4G7 complexes, respectively, for internal validation and to increase angular orientation on the EM grid. The structure of the c2G4-GP complex was solved in the absence of any other antibody, as the complex did not suffer from orientation bias.

c1H3 binds in the vicinity of the glycan cap of GP, similar to c13C6, although the angle of approach is much less steep than that of c13C6 (Fig. 2*B* and Fig. S2*B*). The antibodies c4G7 (Fig. 2*C* and Fig. S2*C*) and c2G4 (Fig. 2*D* and Fig. S2*D*) both bind the base of GP at or near the interface of GP1 and GP2, resembling KZ52 (Fig. S2) (39) and 16F6 (38, 45). c4G7 binds almost perpendicularly to the side of GP, whereas c2G4 binds at the bottom of GP at an upward angle toward GP1.

Our competition binding data indicate that c1H3 and c13C6 compete for binding at the same site on GPΔTM (Fig. 1). To directly compare these two structures, we overlaid the reconstructions of c1H3 and c13C6 and outlined their Fab footprints on GP (Fig. 3*A*). As expected, the antibodies partially but do not

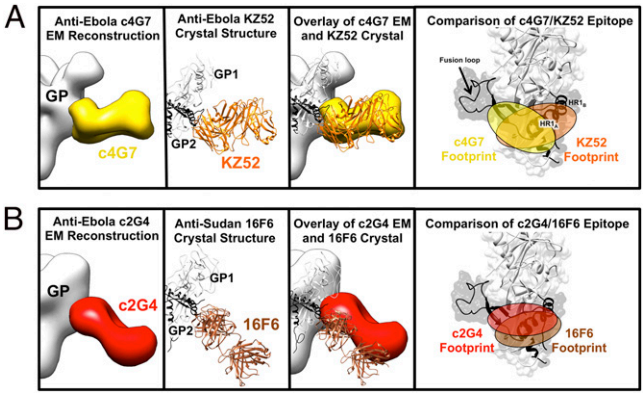

Fig. 4. Comparison of EM reconstructions and crystal structures of mAbs that bind at the GP1-GP2 interface. (*A*) c4G7 (in yellow) binds to a very similar epitope and angle of approach to the human survivor mAb KZ52 (in orange; PDB ID code 3CSY) and their footprints overlap significantly. (*B*) Anti-SUDV mAb 16F6 (in brown; PDB ID code 3VE0) (38, 45) binds a similar epitope to c2G4 (as well as KZ52 and c4G7) and at a similar angle (from the bottom of GP, upward toward GP1), although c2G4 binds closer to GP2 and likely recognizes less of GP1, as previously indicated (28). Note that 16F6 only binds SUDV, whereas the others bind EBOV. Similarity of the binding sites indicates functional conservation across the *ebolavirus* genus.

completely overlap within the glycan cap. A point mutation at W275, shown to prevent binding of c1H3 (22), lies solely within the footprint of c1H3 (Fig. 3*A*).

Our competition binding data indicate that c4G7 and c2G4 indeed compete for binding to the side/base of GP at the GP1–GP2 interface. We also overlaid these structures and mapped their footprints on GP (Fig. 3*B*). Unlike c1H3 and c13C6, the epitopes of c4G7 and c2G4 overlap extensively, and the antibodies differ mainly in their angle of approach to the overlapping binding sites. c2G4 appears to bind almost exclusively to GP2 in the vicinity of $HR1_{A-B}$ (39). c4G7 binds slightly lower on GP, encompassing some of the GP1 base, similar to KZ52 (39). The footprints of both c2G4 and c4G7 shown here, as well as the footprint of KZ52 determined crystallographically, all include residue Q508 of GP2. A point mutation at Q508 has been shown to abolish the binding of c2G4 and c4G7 (22). Here, we show that this same point mutation also abolishes binding of KZ52 (Table S2). Notably, the anti-SUDV antibody 16F6 and an additional anti-Ebola virus mAb, termed ch133 (20, 46, 47), likely bind this site as well. The 16F6 epitope was mapped crystallographically (38, 45); the ch133 epitope is inferred by the mapping of a mutant that escaped it at residue H549 (Fig. 3*B*) (20, 46, 47).

Alignment of the crystal structure of the KZ52–GPΔmuc complex [Protein Data Bank (PDB) ID code 3CSY] (39) with the EM structure of the c4G7:GPΔTM complex indicates that KZ52 and c4G7 bind at a similar angle to GP and have overlapping footprints (Fig. 4*A*). However, KZ52 recognizes a larger portion of $HR1_{A-B}$, whereas c4G7 recognizes an epitope located closer to the base of the fusion loop (Fig. 4*A*).

The angle of binding of c2G4 to GP is more reminiscent of the anti-SUDV mAb 16F6 (19, 38, 45), as the constant regions of both c2G4 and 16F6 mAb are angled toward the viral membrane (Fig. 4*B*). Both c2G4 and 16F6 neutralize well despite their apparent steep angle of approach and proximity to the viral membrane (28, 38). In summary, we now find that at least four antibodies (c2G4, c4G7, KZ52, and 16F6) recognize the GP base and that recognition of the base is a commonality of multiple antibodies that neutralize ebolaviruses.

Discussion

Here we illustrate the structures of four key components of the MB-003, ZMAb, and ZMapp cocktails (Fig. S3), including c13C6 (29), c1H3, c2G4, and c4G7 (28), each bound to Ebola virus GPΔTM (Fig. 2). Among these, two (c13C6 and c1H3) are the first antibodies confirmed to bind within the glycan cap. We compare the four structures of these mAbs to each other (Fig. 3) and also to two mAbs whose structures have previously been solved by X-ray crystallography, namely anti-Ebola KZ52 (39) and anti-SUDV 16F6 (38, 45) (Fig. 4). Overall, we find that antibodies against the ebolaviruses each bind one of three distinct regions (Table S3). These regions, therefore, constitute at least three sites of vulnerability on the viral surface (Fig. 5). Coverage of each of these sites may be important in design of additional therapeutic antibody mixtures against Ebola or related viruses. Similarly, consistent sites of vulnerability have also been noted for other viruses with class I viral glycoproteins, such as HIV-1 and influenza (48, 49).

Some of the anti-ebolavirus antibodies are neutralizing, whereas others are nonneutralizing in vitro but still provide in vivo protection (23, 27, 29). Neutralization is an in vitro assay of the ability of an antibody to block infection in cell culture. We propose that the characteristic of being neutralizing or nonneutralizing may reflect the physical portion of GP that is bound by the antibody. During EBOV entry, the mucin-like domains and glycan caps are removed by cathepsin cleavage before receptor engagement (42, 50–52). Antibodies against the mucin-like domains and glycan caps generally appear nonneutralizing, because they and their epitopes are likely removed from viral particles once those particles are endocytosed and processed, but before receptor binding, which likely happens in late endosomes. Neutralizing antibodies such as KZ52, 16F6, c4G7, and c2G4 could, however, remain attached during GP enzymatic processing. Such antibodies are positioned where they could prevent the structural rearrangements of GP required for viral fusion. Perhaps those nonneutralizing antibodies that are nonetheless protective bind surface expressed GP and facilitate immune responses, such as antibody-dependent cellular cytotoxicity (ADCC) or complement. It has already been demonstrated that ADCC is increased with the plant-derived antibodies of the MB-003 mixture, likely due to the absence of fucose

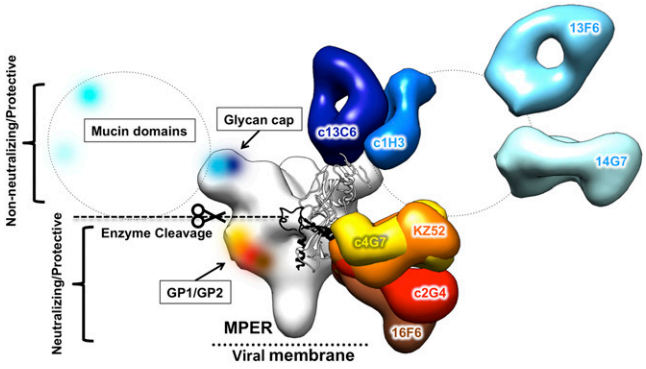

Fig. 5. Sites of vulnerability on Ebola virus for protective mAbs. Anti-Ebola mAbs target key sites on GP. Antibodies that do not neutralize, or that do not neutralize in the absence of complement, bind outside of the core GP in the glycan cap and mucin-like domains, and are shown in cool colors. These antibodies can be protective, despite the removal of these domains before receptor binding in the endosome. All neutralizing mAbs (warm colors) solved to date bind at nearly the same site, within the GP1–GP2 interface. These mAbs bind the core of GP, which remains intact before entry. These mAbs may neutralize the virus by preventing structural changes in GP2 required for membrane fusion. A monomer of GPΔmuc (PDB ID code 3CSY) is fit into the core GP of the c13C6:c4G7 complex. MPER, membrane proximal external region.

on the Fc *N*-glycans (21, 27), which enhances binding by immune effectors.

It is possible that antibody-mediated protection requires a mixture of antibodies that recognize both the core of GP and upper regions. Indeed, the ZMapp cocktail (24), which contains c13C6, c4G7, and c2G4, provides superior protection over MB-003 (21, 23, 27) or ZMAb (22, 24). MB-003 contains only antibodies against domains that are cleaved off GP before viral fusion (Fig. S3*A*). The original ZMAb, and the improved ZMapp, both contain one antibody against the glycan cap plus two against the GP base (Fig. S3 *B* and *C*). The difference between them is that ZMAb contains c1H3 as its glycan cap antibody, whereas ZMapp contains c13C6. Thus, the improved efficacy of ZMapp is likely due to some superiority of c13C6 over c1H3. c13C6 has a different angle of approach that could improve presentation of the Fc for immune effector function (Fig. 3). A remaining question for future studies is if both c4G7 and c2G4 are needed. Our EM maps show that these two antibodies have extensively overlapping epitopes. Future studies will reveal if these antibodies have complementary functions or if it is simply that the right formula is one part anti-glycan cap plus two parts anti-base. Other potential mixtures could be imagined that instead contain one antibody against each of the three major antigenic regions (mucin-like domain, glycan cap, and base) (Fig. 5).

One important consideration for antibody cocktails is whether or not a component antibody or antibodies also bind to sGP. sGP is the soluble, dimeric version of GP that results from the primary ORF of the *GP* gene and is expressed abundantly during EBOV infection (53–55). It has been suggested that antibodies that bind sGP would not be effective in protecting against infection, because sGP could serve as a decoy for antibodies that might otherwise bind viral particles (56, 57). Clearly, however, sGP cross-reactive antibodies such as c1H3 and c13C6 (28, 29) can impart protection and appear to be important components of these mixtures. It is possible that such antibody therapies given in sufficient amounts can surmount the abundance of sGP or that antibodies against sGP interfere with some as-yet-unknown pathogenic function of sGP. Future studies to uncover any shared structural features between sGP and GP and to uncover the mechanism of protection provided by glycan cap-binding antibodies such as c13C6 will be informative for selection and optimization of future antibody therapies.

These studies illustrate that the GP1–GP2 interface in the core of GP is clearly important for protection and elicits multiple potently neutralizing antibodies (39, 45) (Fig. 5). The anti-EBOV antibodies c4G7, c2G4, and KZ52 (Fig. 2*B*) and the anti-SUDV antibody 16F6 overlap significantly in this region (Fig. 3*B*), even though some were raised by vaccination of mice and another in natural infection of a human (Table S3). Further, antibody ch133, which is also protective against Ebola virus, is affected by a point mutation located in this same site (Fig. 3*B*) (46, 47). c4G7, c2G4, KZ52, and 16F6 differ, however, in their angle of approach. KZ52 and c4G7 are shallow and nearly parallel with the viral membrane, whereas c2G4 and 16F6 are steep, with the constant regions angling toward the viral membrane (Fig. 3). It is unclear if the difference in binding angle confers any difference in function. These structures collectively indicate that the GP1–GP2 interface at the base of GP is a major site of vulnerability for Ebola virus, and mAbs that recognize this epitope may be important to include in a therapeutic antibody mixture. Although KZ52 did not provide protection in nonhuman primates as a single mAb (34), it may similarly be effective as a member of an antibody cocktail.

The desperate need for effective pre- and postexposure treatments is further illuminated by the magnitude and persistence of the 2014 Ebola virus outbreak. Strains of Ebola virus currently circulating in Guinea and Sierra Leone bear multiple mutations distinct from previous strains of Ebola virus (58–61). However, our structural modeling indicates that none of the accrued mutations fall directly within the epitopes of the ZMapp antibodies (Fig. S5). Further, ZMapp is able to neutralize previous virulent strains of Ebola (Kikwit outbreak 1995), as well as the current West African 2014 strains (61). These data collectively support that ZMapp would likely have efficacy against viral strains circulating in the ongoing 2014 outbreak. Negative-stain EM and biophysical characterization, which can be done rapidly, can guide the assembly of different mixtures to mitigate viral escape in future strains. Further, this work provides clear next steps to determine if ZMapp can be honed for even greater potency, efficacy, or production.

Materials and Methods

The c13C6, c6D8, h13F6, c1H3, c2G4, and c4G7 Fabs were generated by optimized papain digestion of plant-derived mAbs kindly provided by Mapp Biopharmaceuticals and Kentucky Bioprocessing, which had been engineered, expressed, and purified as previously described (21, 27, 31). Ebola virus GP ectodomains (39, 62) were produced in *Drosophila* Schneider 2 (S2) cells (Invitrogen). All binding experiments were performed using the ForteBio Octet platform. EM reconstructions were carried out by using Xmipp (63) IMAGIC (63), and EMAN2 (64). Fitting of X-ray models into the EM reconstructions was carried out by using UCSF Chimera (65). For more details, see *SI Materials and Methods*.

ACKNOWLEDGMENTS. We thank Dr. Sheik Humarr Khan of Kenema Government Hospital and Dr. Pardis Sabeti of the Broad Institute for sharing unpublished sequence data for the 2014 West African Ebola virus isolates. We thank Dr. Gabriel Lander of The Scripps Research Institute (TSRI) for providing EMAN2 scripts and helpful advice. We also thank Kelsi Swope and Josh Morton from Kentucky Bioprocessing for preparing and sending IgGs. Finally, we thank Dr. Peter Lee and Dr. Gabriel Ozorowski, TSRI, for help with Octet experiments. Electron microscopy was conducted at the National Resource for Automated Molecular Microscopy at TSRI, which is supported by the Biomedical Technology Research Center program (GM103310) of the National Institute of General Medical Sciences. C.D.M. was supported by a predoctoral fellowship from the National Science Foundation, A.B.W. by a Ray Thomas Edwards Foundation award, and E.O.S. by Investigators in the Pathogenesis of Infectious Disease award from the Burroughs Welcome Fund. This work was supported by National Institutes of Health (NIH) Grant R01AI067927 (to E.O.S.) and NIH/National Institute of Allergy and Infectious Diseases Center for Excellence in Translational Research Grant U19AI109762 "Consortium for Immunotherapeutics Against Viral Hemorrhagic Fevers" (to E.O.S., A.B.W., L.Z., and G.P.K.). This is manuscript 28016 from The Scripps Research Institute.

1. Brès P (1978) [The epidemic of Ebola haemorrhagic fever in Sudan and Zaire, 1976: Introductory note]. *Bull World Health Organ* 56(2):245.
2. Jahrling PB, et al. (1990) Preliminary report: Isolation of Ebola virus from monkeys imported to USA. *Lancet* 335(8688):502–505.
3. World Health Organization (2009) Outbreak news. Ebola Reston in pigs and humans, Philippines. *Wkly Epidemiol Rec* 84(7):49–50.
4. Barrette RW, et al. (2009) Discovery of swine as a host for the Reston ebolavirus. *Science* 325(5937):204–206.
5. Falzarano D, Geisbert TW, Feldmann H (2011) Progress in filovirus vaccine development: Evaluating the potential for clinical use. *Expert Rev Vaccines* 10(1): 63–77.
6. Feldmann H, et al. (2007) Effective post-exposure treatment of Ebola infection. *PLoS Pathog* 3(1):e2.
7. Geisbert TW, Bausch DG, Feldmann H (2010) Prospects for immunisation against Marburg and Ebola viruses. *Rev Med Virol* 20(6):344–357.
8. Geisbert TW, et al. (2008) Vesicular stomatitis virus-based ebola vaccine is well-tolerated and protects immunocompromised nonhuman primates. *PLoS Pathog* 4(11): e1000225.
9. Geisbert TW, et al. (2008) Recombinant vesicular stomatitis virus vector mediates postexposure protection against Sudan Ebola hemorrhagic fever in nonhuman primates. *J Virol* 82(11):5664–5668.
10. Marzi A, Feldmann H, Geisbert TW, Falzarano D (2011) Vesicular Stomatitis Virus-Based Vaccines for Prophylaxis and Treatment of Filovirus Infections. *J Bioterror Biodef* S1(4).
11. Côté M, et al. (2011) Small molecule inhibitors reveal Niemann-Pick C1 is essential for Ebola virus infection. *Nature* 477(7364):344–348.
12. Johansen LM, et al. (2013) FDA-approved selective estrogen receptor modulators inhibit Ebola virus infection. *Sci Transl Med* 5(190):190ra179.
13. Warren TK, et al. (2014) Protection against filovirus diseases by a novel broad-spectrum nucleoside analogue BCX4430. *Nature* 508(7496):402–405.

14. Geisbert TW, et al. (2006) Postexposure protection of guinea pigs against a lethal ebola virus challenge is conferred by RNA interference. *J Infect Dis* 193(12): 1650–1657.
15. Geisbert TW, et al. (2010) Postexposure protection of non-human primates against a lethal Ebola virus challenge with RNA interference: A proof-of-concept study. *Lancet* 375(9729):1896–1905.
16. Saphire EO (2013) An update on the use of antibodies against the filoviruses. *Immunotherapy* 5(11):1221–1233.
17. Wong G, Qiu X, Olinger GG, Kobinger GP (2014) Post-exposure therapy of filovirus infections. *Trends Microbiol* 22(8):456–463.
18. Qiu X, Kobinger GP (2014) Antibody therapy for Ebola: Is the tide turning around? *Hum Vaccin Immunother* 10(4):964–967.
19. Dye JM, et al. (2012) Postexposure antibody prophylaxis protects nonhuman primates from filovirus disease. *Proc Natl Acad Sci USA* 109(13):5034–5039.
20. Marzi A, et al. (2012) Protective efficacy of neutralizing monoclonal antibodies in a nonhuman primate model of Ebola hemorrhagic fever. *PLoS ONE* 7(4):e36192.
21. Zeitlin L, et al. (2011) Enhanced potency of a fucose-free monoclonal antibody being developed as an Ebola virus immunoprotectant. *Proc Natl Acad Sci USA* 108(51): 20690–20694.
22. Qiu X, et al. (2012) Successful treatment of ebola virus-infected cynomolgus macaques with monoclonal antibodies. *Sci Transl Med* 4(138):138ra181.
23. Pettitt J, et al. (2013) Therapeutic intervention of Ebola virus infection in rhesus macaques with the MB-003 monoclonal antibody cocktail. *Sci Transl Med* 5(199): ra113.
24. Qiu X, et al. (2014) Reversion of advanced Ebola virus disease in nonhuman primates with ZMapp. *Nature* 514(7520):47–53.
25. Hart MK, Wilson JA, Schmaljohn AL (2003) US Patent 6,630,144 B1.
26. Qiu X, et al. (2012) Ebola GP-specific monoclonal antibodies protect mice and guinea pigs from lethal Ebola virus infection. *PLoS Negl Trop Dis* 6(3):e1575.
27. Olinger GG, Jr, et al. (2012) Delayed treatment of Ebola virus infection with plant-derived monoclonal antibodies provides protection in rhesus macaques. *Proc Natl Acad Sci USA* 109(44):18030–18035.
28. Qiu X, et al. (2011) Characterization of Zaire ebolavirus glycoprotein-specific monoclonal antibodies. *Clin Immunol* 141(2):218–227.
29. Wilson JA, et al. (2000) Epitopes involved in antibody-mediated protection from Ebola virus. *Science* 287(5458):1664–1666.
30. Giritch A, et al. (2006) Rapid high-yield expression of full-size IgG antibodies in plants coinfected with noncompeting viral vectors. *Proc Natl Acad Sci USA* 103(40): 14701–14706.
31. Strasser R, et al. (2008) Generation of glyco-engineered Nicotiana benthamiana for the production of monoclonal antibodies with a homogeneous human-like N-glycan structure. *Plant Biotechnol J* 6(4):392–402.
32. Maruyama T, et al. (1999) Ebola virus can be effectively neutralized by antibody produced in natural human infection. *J Virol* 73(7):6024–6030.
33. Parren PW, Geisbert TW, Maruyama T, Jahrling PB, Burton DR (2002) Pre- and post-exposure prophylaxis of Ebola virus infection in an animal model by passive transfer of a neutralizing human antibody. *J Virol* 76(12):6408–6412.
34. Oswald WB, et al. (2007) Neutralizing antibody fails to impact the course of Ebola virus infection in monkeys. *PLoS Pathog* 3(1):e9.
35. Marzi A, et al. (2013) Antibodies are necessary for rVSV/ZEBOV-GP-mediated protection against lethal Ebola virus challenge in nonhuman primates. *Proc Natl Acad Sci USA* 110(5):1893–1898.
36. Audet J, et al. (2014) Molecular characterization of the monoclonal antibodies composing ZMAb: A protective cocktail against Ebola virus. *Sci Rep* 4:6881.
37. Kajihara M, et al. (2012) Inhibition of Marburg virus budding by nonneutralizing antibodies to the envelope glycoprotein. *J Virol* 86(24):13467–13474.
38. Dias JM, et al. (2011) A shared structural solution for neutralizing ebolaviruses. *Nat Struct Mol Biol* 18(12):1424–1427.
39. Lee JE, et al. (2008) Structure of the Ebola virus glycoprotein bound to an antibody from a human survivor. *Nature* 454(7201):177–182.
40. Lee JE, et al. (2008) Complex of a protective antibody with its Ebola virus GP peptide epitope: Unusual features of a V lambda x light chain. *J Mol Biol* 375(1):202–216.
41. Tran EE, et al. (2014) Spatial localization of the Ebola virus glycoprotein mucin-like domain determined by cryo-electron tomography. *J Virol* 88(18):10958–10962.
42. Lee JE, Saphire EO (2009) Ebolavirus glycoprotein structure and mechanism of entry. *Future Virol* 4(6):621–635.
43. Martinez O, Tantral L, Mulherkar N, Chandran K, Basler CF (2011) Impact of Ebola mucin-like domain on antiglycoprotein antibody responses induced by Ebola virus-like particles. *J Infect Dis* 204(Suppl 3):S825–S832.
44. Olal D, et al. (2012) Structure of an antibody in complex with its mucin domain linear epitope that is protective against Ebola virus. *J Virol* 86(5):2809–2816.
45. Bale S, et al. (2012) Structural basis for differential neutralization of ebolaviruses. *Viruses* 4(4):447–470.
46. Takada A, Ebihara H, Jones S, Feldmann H, Kawaoka Y (2007) Protective efficacy of neutralizing antibodies against Ebola virus infection. *Vaccine* 25(6):993–999.
47. Takada A, et al. (2003) Identification of protective epitopes on ebola virus glycoprotein at the single amino acid level by using recombinant vesicular stomatitis viruses. *J Virol* 77(2):1069–1074.
48. Burton DR, Poignard P, Stanfield RL, Wilson IA (2012) Broadly neutralizing antibodies present new prospects to counter highly antigenically diverse viruses. *Science* 337(6091):183–186.
49. Julien JP, Lee PS, Wilson IA (2012) Structural insights into key sites of vulnerability on HIV-1 Env and influenza HA. *Immunol Rev* 250(1):180–198.
50. Bale S, et al. (2011) Ebola virus glycoprotein needs an additional trigger, beyond proteolytic priming for membrane fusion. *PLoS Negl Trop Dis* 5(11):e1395.
51. Brecher M, et al. (2012) Cathepsin cleavage potentiates the Ebola virus glycoprotein to undergo a subsequent fusion-relevant conformational change. *J Virol* 86(1): 364–372.
52. Chandran K, Sullivan NJ, Felbor U, Whelan SP, Cunningham JM (2005) Endosomal proteolysis of the Ebola virus glycoprotein is necessary for infection. *Science* 308(5728):1643–1645.
53. Barrientos LG, Martin AM, Rollin PE, Sanchez A (2004) Disulfide bond assignment of the Ebola virus secreted glycoprotein SGP. *Biochem Biophys Res Commun* 323(2): 696–702.
54. Sanchez A, et al. (1998) Biochemical analysis of the secreted and virion glycoproteins of Ebola virus. *J Virol* 72(8):6442–6447.
55. Volchkova VA, Feldmann H, Klenk HD, Volchkov VE (1998) The nonstructural small glycoprotein sGP of Ebola virus is secreted as an antiparallel-orientated homodimer. *Virology* 250(2):408–414.
56. Basler CF (2013) A novel mechanism of immune evasion mediated by Ebola virus soluble glycoprotein. *Expert Rev Anti Infect Ther* 11(5):475–478.
57. Mohan GS, Li W, Ye L, Compans RW, Yang C (2012) Antigenic subversion: A novel mechanism of host immune evasion by Ebola virus. *PLoS Pathog* 8(12):e1003065.
58. Baize S, et al. (2014) Emergence of Zaire Ebola virus disease in Guinea. *N Engl J Med* 371(15):1418–1425.
59. Dudas G, Rambaut A (2014) Phylogenetic analysis of Guinea 2014 EBOV Ebolavirus outbreak. *PLoS Curr* 6:6.
60. Calvignac-Spencer S, Schulze JM, Zickmann F, Renard BY (2014) Clock rooting further demonstrates that Guinea 2014 EBOV is a member of the Zaïre lineage. *PLoS Curr* 6:6.
61. Gire SK, et al. (2014) Genomic surveillance elucidates Ebola virus origin and transmission during the 2014 outbreak. *Science* 345(6202):1369–1372.
62. Lee JE, et al. (2009) Techniques and tactics used in determining the structure of the trimeric ebolavirus glycoprotein. *Acta Crystallogr D Biol Crystallogr* 65(Pt 11): 1162–1180.
63. van Heel M, Harauz G, Orlova EV, Schmidt R, Schatz M (1996) A new generation of the IMAGIC image processing system. *J Struct Biol* 116(1):17–24.
64. Tang G, et al. (2007) EMAN2: An extensible image processing suite for electron microscopy. *J Struct Biol* 157(1):38–46.
65. Pettersen EF, et al. (2004) UCSF Chimera—A visualization system for exploratory research and analysis. *J Comput Chem* 25(13):1605–1612.